ORGANISATION EUROPÉENNE POUR LA RECHERCHE NUCLÉAIRE (CERN)
Laboratoire Européen pour la Physique des Particules

CERN-EP/2002-055
15th July 2002

Absolute Lower Limits on the Masses of Selectrons and Sneutrinos in the MSSM

The ALEPH Collaboration*)

Abstract

The results of searches for selectrons, charginos and neutralinos performed with the data collected by the ALEPH detector at LEP at centre-of-mass energies up to 209 GeV are interpreted in the framework of the Minimal Supersymmetric extension of the Standard Model with R-parity conservation. Under the assumptions of gaugino and sfermion mass unification and no sfermion mixing, an absolute lower limit of $73\,\mathrm{GeV}/c^2$ is set on the mass of the lighter selectron $\tilde{\mathrm{e}}_\mathrm{R}$ at the 95% confidence level. Similarly, limits on the masses of the heavier selectron $\tilde{\mathrm{e}}_\mathrm{L}$ and of the sneutrino $\tilde{\nu}_\mathrm{e}$ are set at 107 and $84\,\mathrm{GeV}/c^2$, respectively. Additional constraints are derived from the results of the searches for Higgs bosons. The results are also interpreted in the framework of minimal supergravity.

Submitted to Physics Letters B

*) See next pages for the list of authors

The ALEPH Collaboration

A. Heister, S. Schael

Physikalisches Institut das RWTH-Aachen, D-52056 Aachen, Germany

R. Barate, R. Brunelière, I. De Bonis, D. Decamp, C. Goy, S. Jezequel, J.-P. Lees, F. Martin, E. Merle, M.-N. Minard, B. Pietrzyk, B. Trocmé

Laboratoire de Physique des Particules (LAPP), IN^{2}P^3-CNRS, F-74019 Annecy-le-Vieux Cedex, France

G. Boix,[25] S. Bravo, M.P. Casado, M. Chmeissani, J.M. Crespo, E. Fernandez, M. Fernandez-Bosman, Ll. Garrido,[15] E. Graugés, J. Lopez, M. Martinez, G. Merino, A. Pacheco, D. Paneque, H. Ruiz

Institut de Física d'Altes Energies, Universitat Autònoma de Barcelona, E-08193 Bellaterra (Barcelona), Spain[7]

A. Colaleo, D. Creanza, N. De Filippis, M. de Palma, G. Iaselli, G. Maggi, M. Maggi, S. Nuzzo, A. Ranieri, G. Raso,[24] F. Ruggieri, G. Selvaggi, L. Silvestris, P. Tempesta, A. Tricomi,[3] G. Zito

Dipartimento di Fisica, INFN Sezione di Bari, I-70126 Bari, Italy

X. Huang, J. Lin, Q. Ouyang, T. Wang, Y. Xie, R. Xu, S. Xue, J. Zhang, L. Zhang, W. Zhao

Institute of High Energy Physics, Academia Sinica, Beijing, The People's Republic of China[8]

D. Abbaneo, P. Azzurri, T. Barklow,[30] O. Buchmüller,[30] M. Cattaneo, F. Cerutti, B. Clerbaux,[23] H. Drevermann, R.W. Forty, M. Frank, F. Gianotti, T.C. Greening,[26] J.B. Hansen, J. Harvey, D.E. Hutchcroft, P. Janot, B. Jost, M. Kado,[2] P. Mato, A. Moutoussi, F. Ranjard, L. Rolandi, D. Schlatter, G. Sguazzoni, W. Tejessy, F. Teubert, A. Valassi, I. Videau, J.J. Ward

European Laboratory for Particle Physics (CERN), CH-1211 Geneva 23, Switzerland

F. Badaud, S. Dessagne, A. Falvard,[20] D. Fayolle, P. Gay, J. Jousset, B. Michel, S. Monteil, D. Pallin, J.M. Pascolo, P. Perret

Laboratoire de Physique Corpusculaire, Université Blaise Pascal, IN^{2}P^3-CNRS, Clermont-Ferrand, F-63177 Aubière, France

J.D. Hansen, J.R. Hansen, P.H. Hansen, B.S. Nilsson

Niels Bohr Institute, 2100 Copenhagen, DK-Denmark[9]

A. Kyriakis, C. Markou, E. Simopoulou, A. Vayaki, K. Zachariadou

Nuclear Research Center Demokritos (NRCD), GR-15310 Attiki, Greece

A. Blondel,[12] J.-C. Brient, F. Machefert, A. Rougé, M. Swynghedauw, R. Tanaka H. Videau

Laoratoire Leprince-Ringuet, Ecole Polytechnique, IN^{2}P^3-CNRS, F-91128 Palaiseau Cedex, France

V. Ciulli, E. Focardi, G. Parrini

Dipartimento di Fisica, Università di Firenze, INFN Sezione di Firenze, I-50125 Firenze, Italy

A. Antonelli, M. Antonelli, G. Bencivenni, F. Bossi, G. Capon, V. Chiarella, P. Laurelli, G. Mannocchi,[5] G.P. Murtas, L. Passalacqua

Laboratori Nazionali dell'INFN (LNF-INFN), I-00044 Frascati, Italy

J. Kennedy, J.G. Lynch, P. Negus, V. O'Shea, A.S. Thompson

Department of Physics and Astronomy, University of Glasgow, Glasgow G12 8QQ,United Kingdom[10]

S. Wasserbaech

Department of Physics, Haverford College, Haverford, PA 19041-1392, U.S.A.

R. Cavanaugh,[4] S. Dhamotharan,[21] C. Geweniger, P. Hanke, V. Hepp, E.E. Kluge, G. Leibenguth, A. Putzer, H. Stenzel, K. Tittel, M. Wunsch[19]

Kirchhoff-Institut für Physik, Universität Heidelberg, D-69120 Heidelberg, Germany[16]

R. Beuselinck, W. Cameron, G. Davies, P.J. Dornan, M. Girone,[1] R.D. Hill, N. Marinelli, J. Nowell, S.A. Rutherford, J.K. Sedgbeer, J.C. Thompson,[14] R. White

Department of Physics, Imperial College, London SW7 2BZ, United Kingdom[10]

V.M. Ghete, P. Girtler, E. Kneringer, D. Kuhn, G. Rudolph

Institut für Experimentalphysik, Universität Innsbruck, A-6020 Innsbruck, Austria[18]

E. Bouhova-Thacker, C.K. Bowdery, D.P. Clarke, G. Ellis, A.J. Finch, F. Foster, G. Hughes, R.W.L. Jones, M.R. Pearson, N.A. Robertson, M. Smizanska

Department of Physics, University of Lancaster, Lancaster LA1 4YB, United Kingdom[10]

O. van der Aa, C. Delaere, V. Lemaitre

Institut de Physique Nucléaire, Département de Physique, Université Catholique de Louvain, 1348 Louvain-la-Neuve, Belgium

U. Blumenschein, F. Hölldorfer, K. Jakobs, F. Kayser, K. Kleinknecht, A.-S. Müller, G. Quast,[6] B. Renk, H.-G. Sander, S. Schmeling, H. Wachsmuth, C. Zeitnitz, T. Ziegler

Institut für Physik, Universität Mainz, D-55099 Mainz, Germany[16]

A. Bonissent, P. Coyle, C. Curtil, A. Ealet, D. Fouchez, P. Payre, A. Tilquin

Centre de Physique des Particules de Marseille, Univ Méditerranée, IN^{2}P^3-CNRS, F-13288 Marseille, France

F. Ragusa

Dipartimento di Fisica, Università di Milano e INFN Sezione di Milano, I-20133 Milano, Italy.

A. David, H. Dietl, G. Ganis,[27] K. Hüttmann, G. Lütjens, W. Männer, H.-G. Moser, R. Settles, G. Wolf

Max-Planck-Institut für Physik, Werner-Heisenberg-Institut, D-80805 München, Germany[16]

J. Boucrot, O. Callot, M. Davier, L. Duflot, J.-F. Grivaz, Ph. Heusse, A. Jacholkowska,[32] L. Serin, J.-J. Veillet, J.-B. de Vivie de Régie,[28] C. Yuan

Laboratoire de l'Accélérateur Linéaire, Université de Paris-Sud, IN^{2}P^3-CNRS, F-91898 Orsay Cedex, France

G. Bagliesi, T. Boccali, L. Foà, A. Giammanco, A. Giassi, F. Ligabue, A. Messineo, F. Palla, G. Sanguinetti, A. Sciabà, R. Tenchini,[1] A. Venturi,[1] P.G. Verdini

Dipartimento di Fisica dell'Università, INFN Sezione di Pisa, e Scuola Normale Superiore, I-56010 Pisa, Italy

O. Awunor, G.A. Blair, G. Cowan, A. Garcia-Bellido, M.G. Green, L.T. Jones, T. Medcalf, A. Misiejuk, J.A. Strong, P. Teixeira-Dias

Department of Physics, Royal Holloway & Bedford New College, University of London, Egham, Surrey TW20 OEX, United Kingdom[10]

R.W. Clifft, T.R. Edgecock, P.R. Norton, I.R. Tomalin

Particle Physics Dept., Rutherford Appleton Laboratory, Chilton, Didcot, Oxon OX11 OQX, United Kingdom[10]

B. Bloch-Devaux, D. Boumediene, P. Colas, B. Fabbro, E. Lançon, M.-C. Lemaire, E. Locci, P. Perez, J. Rander, B. Tuchming, B. Vallage

CEA, DAPNIA/Service de Physique des Particules, CE-Saclay, F-91191 Gif-sur-Yvette Cedex, France[17]

N. Konstantinidis, A.M. Litke, G. Taylor

Institute for Particle Physics, University of California at Santa Cruz, Santa Cruz, CA 95064, USA[22]

C.N. Booth, S. Cartwright, F. Combley,[31] P.N. Hodgson, M. Lehto, L.F. Thompson

Department of Physics, University of Sheffield, Sheffield S3 7RH, United Kingdom[10]

A. Böhrer, S. Brandt, C. Grupen, J. Hess, A. Ngac, G. Prange, U. Sieler

Fachbereich Physik, Universität Siegen, D-57068 Siegen, Germany[16]

C. Borean, G. Giannini

Dipartimento di Fisica, Università di Trieste e INFN Sezione di Trieste, I-34127 Trieste, Italy

H. He, J. Putz, J. Rothberg

Experimental Elementary Particle Physics, University of Washington, Seattle, WA 98195 U.S.A.

S.R. Armstrong, K. Berkelman, K. Cranmer, D.P.S. Ferguson, Y. Gao,[29] S. González, O.J. Hayes, H. Hu, S. Jin, J. Kile, P.A. McNamara III, J. Nielsen, Y.B. Pan, J.H. von Wimmersperg-Toeller, W. Wiedenmann, J. Wu, Sau Lan Wu, X. Wu, G. Zobernig

Department of Physics, University of Wisconsin, Madison, WI 53706, USA[11]

G. Dissertori

Institute for Particle Physics, ETH Hönggerberg, 8093 Zürich, Switzerland.

[1]Also at CERN, 1211 Geneva 23, Switzerland.
[2]Now at Fermilab, PO Box 500, MS 352, Batavia, IL 60510, USA
[3]Also at Dipartimento di Fisica di Catania and INFN Sezione di Catania, 95129 Catania, Italy.
[4]Now at University of Florida, Department of Physics, Gainesville, Florida 32611-8440, USA
[5]Also Istituto di Cosmo-Geofisica del C.N.R., Torino, Italy.
[6]Now at Institut für Experimentelle Kernphysik, Universität Karlsruhe, 76128 Karlsruhe, Germany.
[7]Supported by CICYT, Spain.
[8]Supported by the National Science Foundation of China.
[9]Supported by the Danish Natural Science Research Council.
[10]Supported by the UK Particle Physics and Astronomy Research Council.
[11]Supported by the US Department of Energy, grant DE-FG0295-ER40896.
[12]Now at Departement de Physique Corpusculaire, Université de Genève, 1211 Genève 4, Switzerland.
[13]Supported by the Commission of the European Communities, contract ERBFMBICT982874.
[14]Supported by the Leverhulme Trust.
[15]Permanent address: Universitat de Barcelona, 08208 Barcelona, Spain.
[16]Supported by Bundesministerium für Bildung und Forschung, Germany.
[17]Supported by the Direction des Sciences de la Matière, C.E.A.
[18]Supported by the Austrian Ministry for Science and Transport.
[19]Now at SAP AG, 69185 Walldorf, Germany
[20]Now at Groupe d' Astroparticules de Montpellier, Université de Montpellier II, 34095 Montpellier, France.
[21]Now at BNP Paribas, 60325 Frankfurt am Mainz, Germany
[22]Supported by the US Department of Energy, grant DE-FG03-92ER40689.
[23]Now at Institut Inter-universitaire des hautes Energies (IIHE), CP 230, Université Libre de Bruxelles, 1050 Bruxelles, Belgique
[24]Also at Dipartimento di Fisica e Tecnologie Relative, Università di Palermo, Palermo, Italy.
[25]Now at McKinsey and Compagny, Avenue Louis Casal 18, 1203 Geneva, Switzerland.
[26]Now at Honeywell, Phoenix AZ, U.S.A.
[27]Now at INFN Sezione di Roma II, Dipartimento di Fisica, Università di Roma Tor Vergata, 00133 Roma, Italy.
[28]Now at Centre de Physique des Particules de Marseille, Univ Méditerranée, F-13288 Marseille, France.
[29]Also at Department of Physics, Tsinghua University, Beijing, The People's Republic of China.
[30]Now at SLAC, Stanford, CA 94309, U.S.A.
[31]Deceased

1 Introduction

Supersymmetry [1] predicts the existence of a supersymmetric partner for each Standard Model particle chirality state. In this letter, the results of standard searches for sleptons ($\tilde{\ell}$) and charginos ($\chi^{\pm}$) in $\mathrm{e^+e^-}$ collisions, already reported by ALEPH in Refs. [2, 3, 4], are combined with those of selectron and neutralino searches specifically developed for final states not considered in the former analyses. The results of these searches allow an absolute lower limit to be set on the selectron and sneutrino mass.

The theoretical framework is the Minimal Supersymmetric extension of the Standard Model (MSSM) [1], with R-parity conservation and the assumption that the lightest supersymmetric particle (LSP) is the lightest neutralino χ^0_1. The notations and conventions of Ref. [3] are used for the MSSM parameters. The interpretation of the results in terms of mass limits is done under the assumption of gaugino and sfermion mass unification to common gaugino and scalar masses, $m_{1/2}$ and m_0, at the GUT scale. At the electroweak scale, gaugino masses are determined at tree level by $m_{1/2}$, the Higgs mass term μ and $\tan\beta$, the ratio of vacuum expectation values of the two Higgs doublets, assumed to be greater than 1 as is usual in the MSSM.

Charged and neutral slepton masses are expressed as indicated in Eqs. (1–3), from which it can be seen that the supersymmetric partner of the right-handed electron $\tilde{\mathrm{e}}_{\mathrm{R}}$ is the lighter of the two selectrons.

$$m^2_{\tilde{\ell}_{\mathrm{R}}} = m_0^2 + 0.15\, m^2_{1/2} - m^2_{\mathrm{Z}} \cos 2\beta \sin^2\theta_{\mathrm{W}} \quad (1)$$

$$m^2_{\tilde{\ell}_{\mathrm{L}}} = m_0^2 + 0.52\, m^2_{1/2} - \frac{m^2_{\mathrm{Z}}}{2} \cos 2\beta \left(1 - 2\sin^2\theta_{\mathrm{W}}\right) \quad (2)$$

$$m^2_{\tilde{\nu}} = m_0^2 + 0.52\, m^2_{1/2} + \frac{m^2_{\mathrm{Z}}}{2} \cos 2\beta \quad (3)$$

Mixing effects, proportional to the mass of the Standard Model partner, are expected to be small for selectrons, and are therefore neglected throughout. For the results obtained in the MSSM, the mixing is set to zero for all sfermions by enforcing the parameters A_{f} to their no-mixing values, $A_{\mathrm{f}} = \mu\tan\beta$ or $\mu\cot\beta$ for down-type and up-type sfermions, respectively.

The results of Higgs boson searches [5] are exploited to further constrain the selectron and sneutrino masses at small $\tan\beta$ values, for any values of the pseudoscalar neutral Higgs boson mass m_{A} and of A_{t}, the trilinear coupling in the stop sector.

Tighter limits are also set in the framework of a highly constrained MSSM version known as minimal supergravity (mSUGRA) [1]. In this model, m_{A} also derives from the common scalar mass m_0 at the GUT scale, the value $|\mu|$ is predicted from dynamical electroweak symmetry breaking, and the trilinear coupling at the GUT scale, A_0, is common to all sfermions. In this letter, $A_0 = 0$ is assumed.

The data used in the analyses entering the present combination were collected with the ALEPH detector at LEP, at centre-of-mass energies ranging from 183 to 209 GeV. The corresponding integrated luminosities are given in Table 1. The results of the dedicated

searches for selectrons and neutralinos in the data collected in the year 2000 are reported in this letter. These selections address

(i) the $\tilde{e}_R\tilde{e}_L$ production to investigate, as described in Ref. [6], small mass differences between $\tilde{e}_R$ and χ_1^0, for which the selections of Ref. [2] become ineffective;

(ii) the $\chi_1^0\chi_3^0$ production with a subsequent neutralino decay into slepton $\chi_3^0 \to \tilde{\ell}_R\ell$, to cover specific regions of the MSSM parameter space in which none of the selections of Refs. [2, 3, 4, 6] constrain the mass of the selectron.

This letter is organized as follows. In Section 2, the search strategy towards an absolute lower limit on the selectron and sneutrino masses is explained. The ALEPH detector is briefly described in Section 3. The selections developed for the two specific final states mentioned above are presented in Section 4, and the interpretation of their results, combined with those of previous analyses, is given in Section 5.

All limits reported in this letter are at the 95% confidence level.

Table 1: Integrated luminosities collected between 1997 and 2000 and average centre-of-mass energies.

Year	1997	1998	1999				2000		
$\sqrt{s}$ (GeV)	182.7	188.6	191.6	195.5	199.5	201.6	205.2	206.6	208.0
$\mathcal{L}$ (pb^{-1})	56.8	173.6	28.9	79.8	86.2	42.0	75.3	122.6	9.4

2 Search strategy

An absolute lower limit on the lighter selectron mass can be derived by a scan of the MSSM parameters, m_0, $m_{1/2}$, $\tan\beta$ and μ. In the absence of sfermion mixing, these parameters suffice to determine the masses and couplings of gauginos and sleptons at tree level, and therefore the relevant production cross sections and decay branching fractions. The scan is performed for $\tan\beta$ between 1 and 50, and μ between -10 and $+10\,\mathrm{TeV/c^2}$. For m_0 and $m_{1/2}$, the explored range is limited to values smaller than from 100 to 200 GeV/c^2 to keep the selectron masses below the LEP kinematic limit. The scan of $m_{1/2}$ is further bounded from below by the absolute lower limit on the mass of the LSP, set at 37 GeV/c^2 in Ref. [3] under the same hypotheses as those used in this letter.

For large mass differences ΔM ($\Delta M \gtrsim 10$ GeV/c^2) between the lighter selectron and the lightest neutralino, the standard $\tilde{e}_R\tilde{e}_R$ searches [2] apply as long as selectrons decay predominantly into $e\chi_1^0$, and allow selectron masses to be excluded beyond 90 GeV/c^2. The efficiency of this selection decreases with ΔM. Indeed, for small ΔM values (below 4 GeV/c^2), the searches can barely improve on the limit obtained from the Z width measurement at LEP 1 [7].

However, this case can be covered as described in Ref. [6] by a search for the $\tilde{e}_R\tilde{e}_L$ associated production, with the subsequent decay of both sparticles into $e\chi_1^0$. In this final state, at least one energetic electron stems from the decay of the heavier selectron. For ΔM values in excess of $\sim 2\,\mathrm{GeV}/c^2$, the additional low-momentum electron remains visible. The standard selectron searches are therefore efficient at selecting the $\tilde{e}_R\tilde{e}_L$ production by merely adapting the electron momentum sliding cuts as a function of the lighter selectron and neutralino masses. For very small ΔM values, the low momentum electron is not reconstructed, such that the final state consists of a single electron and missing energy. The results of the search for this topology, investigated in Ref. [6] and updated at centre-of-mass energies up to 202 GeV in Ref. [3], are reported here at the highest energies produced by LEP 2 in the year 2000.

In large parts of the parameter space, the lower limit on the selectron mass is set by using a combination of the above-mentioned selectron searches. Problems occur in certain regions characterized by small values of $\tan\beta$, $|\mu|$ and m_0, which lead to light χ_2^0 with a high photino field content. Predominant selectron cascade decays via the χ_2^0 yield final states not selected by the standard selectron searches. In this case, the charginos are also light such that the region is in general excluded by chargino searches. This coverage vanishes in the so called *corridor* [3], a subset of model parameters for which the chargino and the sneutrino are degenerate in mass. In the corridor, the final state arising from the chargino two-body (2B) decay into $\tilde{\nu}\ell$, dominant over the three-body (3B) decay into $\chi_1^0 f\bar{f}$, is in practice invisible.

In this case, though, the χ_3^0 is light enough for the $\chi_1^0\chi_3^0$ production cross section with a χ_3^0 decay into $\tilde{\ell}\ell$ to be sufficient to cover this peculiar region. Searches for six different final states, according to the slepton decay (direct or cascade) and flavour (e or μ), were developed to address the associated neutralino production, and their results are reported here.

The low-$\tan\beta$ region is also covered by the result of the searches for the lighter neutral scalar Higgs boson h [5], as described in Ref. [3]. However, because the lower limit on $\tan\beta$ varies rapidly with the top quark mass through radiative corrections to m_h, the uncertainty on m_{top} renders this indirect limit less robust than that obtained with the direct selectron searches.

3 The ALEPH detector

A thorough description of the ALEPH detector and its performance as well as of the standard reconstruction and analysis algorithms can be found in Refs. [8, 9]. Only a brief summary is given here.

The trajectories of charged particles are measured by a silicon vertex detector, a cylindrical multi-wire drift chamber and a large time projection chamber (TPC). Charged particle trajectories are called *good tracks* if they are reconstructed with at least four space points in the TPC, a transverse momentum in excess of $200\,\mathrm{MeV}/c$, a polar angle with respect to the beam such that $|\cos\theta| < 0.95$, and if they originate from within a

cylinder of length 20 cm and radius 2 cm coaxial with the beam and centred at the nominal interaction point. In addition, good tracks must not be compatible with arising from a photon conversion to e^+e^- identified as pairs of oppositely-charged particles satisfying stringent conditions on their distance of closest approach and their invariant mass.

The tracking devices are immersed in an axial magnetic field of 1.5 T, provided by a superconducting solenoidal coil and surrounded by a highly segmented electromagnetic calorimeter (ECAL). The ECAL is used to identify electrons and photons by the characteristic longitudinal and transverse developments of the associated showers, and is supplemented for low momentum electrons by the measurement in the TPC of the specific energy loss by ionization.

The iron return yoke is instrumented with streamer tubes as a hadron calorimeter (HCAL). It provides a measurement of the hadronic energy and, together with external muon chambers, efficient identification of muons by their characteristic penetration pattern. Luminosity monitors extend the calorimeter coverage down to 34 mrad.

Global event quantities such as total energy, transverse momentum or missing energy, are determined from an energy-flow algorithm which combines all the above measurements into charged particles (electrons, muons, charged hadrons), photons and neutral hadrons, which are the basic objects used in the selections presented in this letter.

4 Event Selection

The selection criteria described below were optimized with the $\bar{N}_{95}$ prescription [10] which consists in minimizing the upper limit on the signal cross section expected in the absence of signal processes. To do so, the selections were applied to fully simulated standard model background samples, generated as in Ref. [2] for $e^+e^- \to f\bar{f}$, WW, ZZ, Zee, Weν, Z$\nu\bar{\nu}$, and for $\gamma\gamma$ interactions. The simulation of the associated $\tilde{e}_R\tilde{e}_L$ and $\chi_1^0\chi_3^0$ production was performed with SUSYGEN [11].

4.1 Update of the search for associated $\tilde{e}_R\tilde{e}_L$ production

The selection of single-electron final states, described in detail in Ref. [6], was applied to the highest centre-of-mass energy data, with the kinematic cuts appropriately rescaled. The numbers of candidate events observed and background events expected are given in Table 2, together with the results of previous years [3, 6, 12].

The total number of events in the data is significantly smaller than expected from standard background sources, dominated by the processes $e^+e^- \to$ Weν and $e^+e^- \to$ Zee. A study of this 2.2 standard deviation deficit led to the conclusion that it is unlikely to be of systematic origin. In particular, the distributions of all relevant kinematic quantities are in qualitative agreement with those expected from the production of the Weν and the Zee final states as is exemplified in Fig. 1 for the total and the transverse momentum of the leading electron at centre-of-mass energies in excess of 188.6 GeV. The total cross

Table 2: Numbers of candidate events observed ($N_{\rm obs}$) and background events expected ($N_{\rm exp}$) for the single-electron selection.

Energy (GeV)	$N_{\rm exp}$	$N_{\rm obs}$
182.7	6.6	5
188.6	13.8	8
191.6	2.7	2
195.5	7.5	9
199.5	8.2	9
201.6	4.2	2
205.2	7.7	5
206.6	13.8	7
208.0	1.0	0
Total	65.5	47

sections predicted for $e^+e^- \to We\nu$ by several generators (PYTHIA [13], GRACE4F [14]) show no difference beyond the 10% level, which would account for only a third of the effect. Notwithstanding the probable statistical origin of this deficit, it is conservatively taken into account in deriving signal cross-section upper limits as is explained in Section 5.1.

4.2 Search for associated $\chi^0_1\chi^0_3$ production

The χ^0_3 decay modes considered in the present analysis are listed in Table 3. The χ^0_3 decay via selectrons or smuons leads to final states with electrons, muons and possibly photons. The selection criteria used in these analyses are based on the acoplanar lepton or single electron analyses. The selection cuts are optimized and adapted for each specific decay topology. The number of good tracks in the detector depends on the decay mode and on the mass differences involved.

- In decay mode A, one or two good tracks (electrons or muons) are expected. The acoplanar lepton and the single electron searches are therefore applied as preselections with no modification. The latter is extended to also cover the single muon topology, by substituting muon identification for electron identification.

- In decay mode B, the χ^0_3 decay yields a high momentum lepton and typically three softer leptons. For large $\Delta M_{\chi^0_2\chi^0_1}$ at least three good tracks (electrons or muons) are required, and the acoplanar lepton search is applied as a preselection on the two leading tracks. The single-electron or single-muon selections, modified to accept up to three low momentum tracks, bring additional efficiency for small $\Delta M_{\chi^0_2\chi^0_1}$ and $\Delta M_{\tilde{\ell}_{\rm R}\chi^0_2}$ values.

Table 3: Leptonic χ_3^0 decay modes and final states. In the present analysis only decay modes via selectrons and smuons are considered.

decay mode									final state
A	χ_3^0	$\rightarrow$	$\tilde{\ell}_{\mathrm{R}}$	$+$	ℓ				one or two leptons
			$\tilde{\ell}_{\mathrm{R}}$	$\rightarrow$	χ_1^0	$+$	ℓ		
B	χ_3^0	$\rightarrow$	$\tilde{\ell}_{\mathrm{R}}$	$+$	ℓ				one to four leptons
			$\tilde{\ell}_{\mathrm{R}}$	$\rightarrow$	χ_2^0	$+$	ℓ		
					χ_2^0	$\rightarrow$	$\chi_1^0 + \ell\ell$		
C	χ_3^0	$\rightarrow$	$\tilde{\ell}_{\mathrm{R}}$	$+$	ℓ				one or two leptons
			$\tilde{\ell}_{\mathrm{R}}$	$\rightarrow$	χ_2^0	$+$	ℓ		and a photon
					χ_2^0	$\rightarrow$	$\chi_1^0 + \gamma$		

- In decay mode C, one or two good tracks are expected, accompanied with an energetic photon. The acoplanar-lepton and the single-lepton selections are therefore applied, modified by requiring a photon with an energy in excess of 5 GeV. Furthermore, its angular separation and invariant mass with any good track must be larger than 10° and 2 GeV/c^2, respectively.

Because of the specific kinematics of the final states arising from $\chi_1^0\chi_3^0$, other common requirements are applied. In particular, the presence of two invisible χ_1^0's leads to large missing energy. To reduce the dominant backgrounds from WW and ZZ processes, the visible mass is therefore required to be smaller than $80\,\mathrm{GeV}/c^2$. Moreover, as the leading lepton is expected to be more energetic in $\chi_1^0\chi_3^0$ production than in direct selectron production, the cuts on its momentum p_1 and its transverse momentum p_{T1} are significantly tightened. The additional background from $\gamma\gamma$ processes selected with three or four good tracks is efficiently reduced by these cuts. Finally, the acoplanarity cut (Φ_{aco}) is relaxed in some cases to preserve a reasonable signal efficiency. The basic selections and the additional/modified criteria for each of the final states are summarized in Table 4.

The numbers of candidate events observed (N_{obs}) and background events expected (N_{exp}) for the three analyses are given in Table 5.

The results of analysis A are similar to those described in Ref. [2] and in Section 4.1 for the slepton searches. The selection of three to four leptons in analysis B yields only a small number of expected background and candidate events. The deficit in the selection of 1(+3) leptons is correlated to that in the single-electron selection presented in Section 4.1. In analysis C, the background expectation is strongly suppressed by the requirement of a high-energy photon in the final state.

Finally, sliding cuts on the momenta of the leading two leptons are applied as a function of $m_{\tilde{\ell}}$ and m_{χ^0}. These cuts are defined by the momentum ranges expected for the kinematics of the decay chain involved.

Table 4: Selection criteria for the three $\chi_1^0\chi_3^0$ decay modes A, B and C for different final states. The numbers of additional good tracks with low momentum are indicated in brackets for each of the final states.

	Signature	Basic Selection	Modified Cuts
A	2 ℓ	Acoplanar Leptons	$M_{\rm vis} < 80\,\mathrm{GeV}/c^2$, $p_1 > 6\%\sqrt{s}$
	1(+1) ℓ	Single Electron	Selection extended to single muons
B	3-4 ℓ	Acoplanar Leptons	Three to four good tracks Standard cuts on the two leading tracks $M_{\rm vis} < 80\,\mathrm{GeV}/c^2$, $p_1 > 8\%\sqrt{s}$
	1(+3) ℓ	Single Lepton (A)	$p_{\rm T1} > 10\%\sqrt{s}$, Energy of additional good tracks $< 2\%\sqrt{s}$ In case of $\geq$ 2 good tracks: $M_{\rm vis} > 4\%\sqrt{s}$, $\Phi_{\rm aco} < 170^\circ$
C	2ℓ+γ	Acoplanar Leptons	One isolated γ (see text), $E_\gamma > 5\,\mathrm{GeV}$, $p_{\rm T1} > 8\,\mathrm{GeV}/c$, $M_{\rm vis} < 80\,\mathrm{GeV}/c^2$
	1(+1)ℓ+γ	Single Lepton (A)	One isolated γ (see text), $E_\gamma > 5\,\mathrm{GeV}$, For one good track: $p_1 < 46.5\%\sqrt{s}$, $\Phi_{\rm aco} < 175^\circ$

5 Results

5.1 Systematic uncertainties and cross section upper limits

The main systematic uncertainties on the background and signal predictions arise from the statistics of the simulated samples and from the simulation of the lepton identification [2]. Both the background and signal expectations are conservatively reduced by this uncertainty. The predicted background contribution from $e^+e^- \to We\nu$ is further reduced by 10 % to account for the theoretical uncertainty of the production cross section. A systematic correction of -14% is also applied on the signal efficiencies to account for the effect of the cut on the energy detected at small polar angle [2].

The optimal combination of selections is chosen according to the $\bar{N}_{95}$ prescription for each set of MSSM parameters tested. To derive cross section upper limits, the dominant background ($e^+e^- \to$ WW for the selections based on the acoplanar-lepton search, and $e^+e^- \to$ Zee and Weν for those based on the single-track search) is subtracted with the method of Ref. [15].

5.2 Limit on $m_{\tilde{\rm e}_{\rm R}}$

In the MSSM framework, the upper bounds on the cross section allow lower limits to be set on the lighter selectron mass with a scan of the four relevant parameters, m_0, $m_{1/2}$,

Table 5: Numbers of candidate events observed ($N_{\rm obs}$) and background events expected ($N_{\rm exp}$) for the $\chi^0_1\chi^0_3$ selections in the year 2000 data set.

	Signature	$N_{\rm exp}$	$N_{\rm obs}$
A	2 e	16.5	18
	2 μ	15.0	23
	1(+1) e	22.5	12
	1(+1) μ	13.7	9
B	3-4 ℓ	4.4	2
	1(+3) ℓ	33.6	17
C	2ℓ+γ	2.1	3
	1(+1)ℓ+γ	3.8	4

μ and $\tan\beta$, as described in Section 2. These limits are presented here in the (m_0, $m_{1/2}$) plane.

For large $\tan\beta$ values (in excess of ~ 7), small differences ΔM between the $\tilde{\rm e}_{\rm R}$ and χ^0_1 masses are only allowed for large χ^0_1 masses. Any selectron mass below $92\,{\rm GeV}/c^2$ is therefore excluded by the standard $\tilde{\rm e}_{\rm R}\tilde{\rm e}_{\rm R}$ searches in this region of the parameter space.

For smaller $\tan\beta$ values, small ΔM occur at lower χ^0_1 masses and the limit set by $\tilde{\rm e}_{\rm R}\tilde{\rm e}_{\rm R}$ searches therefore becomes less stringent. For $\tan\beta$ values smaller than 2.6, the single electron search takes over, as long as $|\mu|$ remains greater than $70\,{\rm GeV}/c^2$. The smallest non-excluded selectron mass, $m_{\tilde{\rm e}_{\rm R}} = 73\,{\rm GeV}/c^2$, is found in this region ($\tan\beta = 1.5$ and $\mu = -5\,{\rm TeV}/c^2$), for $m_{1/2} = 179\,{\rm GeV}/c^2$ and $m_0 = 2\,{\rm GeV}/c^2$, as displayed in Fig. 2.

Small negative values of μ are in general excluded by either chargino searches or neutralino searches for any selectron mass value. An example is shown in Fig. 3 where the exclusion domains in the (m_0, $m_{1/2}$) plane are given for $\tan\beta = 1.0$ and $\mu = -45\,{\rm GeV}/c^2$ with and without the dedicated neutralino searches. It can be seen that the additional $\chi^0_1\chi^0_3$ searches allow the chargino corridor to be covered. The overall limit on $m_{\tilde{\rm e}_{\rm R}}$ is therefore set by the $\tilde{\rm e}_{\rm R}\tilde{\rm e}_{\rm L}$ analysis at larger negative values of μ where the $m_{1/2}$ coverage of the chargino searches is reduced due to larger chargino and neutralino masses.

The limit on $m_{\tilde{\rm e}_{\rm R}}$ is shown in Fig. 4 as a function of $\tan\beta$. Each point represents the result of a scan over μ, $m_{1/2}$ and m_0, allowing an absolute lower limit on the selectron mass to be set at $m_{\tilde{\rm e}_{\rm R}} > 73\,{\rm GeV}/c^2$.

5.3 Limits on $m_{\tilde{\nu}}$ and $m_{\tilde{\rm e}_{\rm L}}$

The present analysis can also be used to derive limits on the masses of the heavier selectron and the sneutrino, exploiting the relations given in Eqs. (2) and (3). For a given value of $\tan\beta$, $m_{\tilde{\rm e}_{\rm L}}$ and $m_{\tilde{\nu}}$ take their minimal values for the same parameter combination, because the difference between the masses of these two sparticles is only a function of

$\tan\beta$. Because the $m_{1/2}$ dependence is stronger for $m_{\tilde{e}_L}$ and $m_{\tilde{\nu}}$ than for $m_{\tilde{e}_R}$, the limits are found at smaller values of $m_{1/2}$ and larger values of m_0. In general, these limits are located at the intersection of the exclusion borders of the selectron and chargino searches or, for $\tan\beta < 1.5$, at the selectron exclusion-border for $m_{\chi_1^0} = 37\,\mathrm{GeV}/c^2$ [3].

The lower limits on $m_{\tilde{e}_L}$ and $m_{\tilde{\nu}}$ are shown in Fig. 5 as a function of $\tan\beta$. The basic shape reflects the opposite $\tan\beta$-dependence of $m_{\tilde{e}_L}$ and $m_{\tilde{\nu}}$. The overall limit for the heavier selectron is found to be $m_{\tilde{e}_L} > 107\,\mathrm{GeV}/c^2$ for $\tan\beta = 1.0$ and $\mu = -80\,\mathrm{GeV}/c^2$. For the sneutrinos, an overall limit of $m_{\tilde{\nu}} > 84\,\mathrm{GeV}/c^2$ is obtained for $\tan\beta > 10$ and $\mu \leq -1000\,\mathrm{GeV}/c^2$.

5.4 Constraints from Higgs boson searches

As explained in Ref. [3], a lower limit on the mass of the lightest CP-even Higgs boson (m_h) can be translated into a lower limit on $m_{1/2}$ as a function of $\tan\beta$ for a given value of m_0. The A boson mass m_A and the stop mixing, controlled by $(A_t - \mu\cot\beta)$, are chosen in a way that maximizes m_h for a given set of $m_{1/2}$, m_0 and $\tan\beta$. The limit on $m_{1/2}$ decreases with increasing m_0. Therefore, the choice $m_0 = 100$ GeV/c^2, corresponding to the kinematic limit for selectron production (Eq. 1), is conservative for the present analysis.

The limit becomes less stringent with increasing m_{top}. The impact of the m_{top} uncertainty ($\pm 5\,\mathrm{GeV}/c^2$) is estimated by performing the calculation for $m_{\mathrm{top}} = 175$ and $180\,\mathrm{GeV}/c^2$. The results are obtained with the ALEPH lower limit on m_h [5]. The limit on $m_{1/2}$ decreases rapidly with increasing $\tan\beta$, hence the impact of the Higgs boson searches on the present results is sizeable only for small $\tan\beta$.

The resulting lower limits on $m_{\tilde{e}_R}$, $m_{\tilde{e}_L}$ and $m_{\tilde{\nu}}$ are shown in Figs. 4 and 5 for $m_{\mathrm{top}} = 175\ (180)\,\mathrm{GeV}/c^2$. The overall limit on $m_{\tilde{e}_R}$ is found at $\tan\beta = 2.8(2.4)$, $m_{\tilde{e}_R} > 77(75)\,\mathrm{GeV}/c^2$. The limit on $m_{\tilde{e}_L}$ is found to be $m_{\tilde{e}_L} > 115(115)\,\mathrm{GeV}/c^2$. Since the limit on $m_{\tilde{\nu}}$ is found at large $\tan\beta$, the constraints from Higgs boson searches have no impact in this case.

5.5 Interpretation in mSUGRA

The results of the searches for selectrons, charginos, neutralinos and Higgs bosons are also combined within the framework of minimal supergravity, following the analysis presented in Ref. [3]. Scans of the $(m_0, m_{1/2})$ plane are performed as a function of $\tan\beta$, for both signs of μ and for $A_0 = 0$.

The results of the neutral Higgs boson searches [5] are interpreted for hZ, HZ and hA production, where h and H are, respectively, the lighter and the heavier CP-even Higgs bosons, and A the CP-odd Higgs boson.

In minimal supergravity, the trilinear couplings A_τ, A_b and A_t are unambiguously predicted from the model parameters. Mixing effects can therefore not be arbitrarily

switched off as is done in the previous sections. While mixing in the squark sector is relevant only for the Higgs boson mass and coupling prediction, mixing in the stau sector can lead to a stau much lighter than selectrons and smuons, thus affecting the decay phenomenology of charginos, neutralinos and Higgs bosons. Decays into staus may indeed become predominant and lead to final state topologies with taus. These topologies are not always efficiently covered by the searches described in the previous sections, in particular if the mass difference between the lightest neutralino and the stau is small. Three additional searches are used to address this new situation:

1. the search for the associated neutralino production $e^+e^- \to \chi^0_2\chi^0_1$ with the subsequent decay $\chi^0_2 \to \tilde{\tau}\tau \to \chi^0_1\tau\tau$ [4], leading to at least one visible τ in the final state;

2. the search for an invisible Higgs boson [5], which covers the $e^+e^- \to hZ$ process followed by the decay $h \to \tilde{\tau}\tilde{\tau} \to \chi^0_1\chi^0_1\tau\tau$;

3. the search for heavy stable charged particles [18] which addresses the stau-pair production $e^+e^- \to \tilde{\tau}\tilde{\tau}$ when the mass difference with the LSP is smaller than m_τ.

The impact of each of the analyses (standard and additional) in the $(m_0, m_{1/2})$ plane is illustrated in Figs. 6a to 6d for two typical $\tan\beta$ values, $\tan\beta = 15$ and 30, and for both signs of μ. In general, small $m_{1/2}$ values are excluded by selectron and Higgs boson searches. Small m_0 values either are theoretically forbidden or correspond to a stau LSP.

The excluded domains in the $(m_0, m_{1/2})$ plane can be translated into lower limits on $m_{\tilde{e}_R}$, $m_{\tilde{e}_L}$ and $m_{\tilde{\nu}}$, shown in Fig. 7 as a function of $\tan\beta$, for $m_{\rm top} = 175\,\mathrm{GeV}/c^2$ and for both signs of μ. With increasing $\tan\beta$, the domains covered by Higgs boson searches shrink, while the regions with a stau LSP extend because of mixing effects in the stau sector. The minimal combined exclusion is reached for intermediate $\tan\beta$ values, around 15. The structure at large $\tan\beta$ is due to a loss of sensitivity of the combined search for the hZ and HZ processes. As can be seen in the example shown in Fig. 6e, a non-excluded channel of the $(m_0, m_{1/2})$ plane opens up, in which the hZ coupling is too small and the H mass too large for the hZ and HZ production to contribute significantly.

Altogether, a lower limit on the selectron mass of 95 GeV/c^2 is derived for $A_0 = 0$ and for both signs of μ. For the heavier selectron and the sneutrino, mass lower limits of 152 and 130 GeV/c^2 are obtained, respectively.

6 Conclusions

The results of searches for selectron, chargino and neutralino production in the data collected by ALEPH at centre-of-mass energies up to 209 GeV have been interpreted in the framework of the MSSM with R-parity conservation, gaugino and sfermion mass unification, and no sfermion mixing. A scan over the four parameters $\tan\beta, \mu, m_{1/2}$ and

m_0 has been performed to determine the following lower limits on the masses of selectrons and sneutrinos:

$$m_{\tilde{\mathrm{e}}_\mathrm{R}} > 73\,\mathrm{GeV}/c^2,$$
$$m_{\tilde{\mathrm{e}}_\mathrm{L}} > 107\,\mathrm{GeV}/c^2,$$
$$m_{\tilde{\nu}} > 84\,\mathrm{GeV}/c^2.$$

These limits improve on earlier results obtained at lower centre-of-mass energies by the L3 collaboration [19].

The limits on the selectron masses can be further improved by including constraints from Higgs boson searches. The results depend slightly on the value of the top quark mass. For $m_{\mathrm{top}} = 175(180)\ \mathrm{GeV}/c^2$, mass limits of

$$m_{\tilde{\mathrm{e}}_\mathrm{R}} > 77(75)\,\mathrm{GeV}/c^2,$$
$$m_{\tilde{\mathrm{e}}_\mathrm{L}} > 115(115)\,\mathrm{GeV}/c^2$$

are obtained.

Within minimal supergravity, mass lower limits have been set at

$$m_{\tilde{\mathrm{e}}_\mathrm{R}} > 95\,\mathrm{GeV}/c^2,$$
$$m_{\tilde{\mathrm{e}}_\mathrm{L}} > 152\,\mathrm{GeV}/c^2,$$
$$m_{\tilde{\nu}} > 130\,\mathrm{GeV}/c^2,$$

for $A_0 = 0$ and $m_{\mathrm{top}} = 175\,\mathrm{GeV}/c^2$.

Acknowledgements

It is a pleasure to congratulate our colleagues from the accelerator divisions for the outstanding operation of LEP 2, especially in its last year of running during which the accelerator performance were pushed beyond expectation. We are indebted to the engineers and technicians in all our institutions for their contributions to the excellent performance of ALEPH. Those of us from non-member states wish to thank CERN for its hospitality and support.

References

[1] H.P. Nilles, Phys. Rep. **110** (1984) 1;
H.E. Haber and G.L. Kane, Phys. Rep. **117** (1985) 75.

[2] ALEPH Coll., "*Search for scalar leptons in e^+e^- collisions at centre-of-mass energies up to 209 GeV*", Phys. Lett. **B526** (2002) 206.

[3] ALEPH Coll., "*Search for supersymmetric particles in e^+e^- collisions at $\sqrt{s}$ up to 202 GeV and mass limit for the lightest neutralino* ", Phys. Lett. **B499** (2001) 67.

[4] ALEPH Coll., "*Results on Chargino and Neutralino Searches in e^+e^- collisions up to $\sqrt{s}$ = 209 GeV and Mass Limit for the Lightest Neutralino including stau mixing* ", paper in preparation.

[5] ALEPH Coll., "*Final results of the searches for neutral Higgs bosons in e^+e^- collisions at $\sqrt{s}$ up to 209 GeV* ", Phys. Lett. **B526** (2002) 191.

[6] ALEPH Coll., "*Search for sleptons in e^+e^- collisions at centre-of-mass energies up to 184 GeV* ", Phys. Lett. **B433** (1998) 176.

[7] ALEPH Coll., "*Searches for new particles in Z decays using the ALEPH detector* ", Phys. Rep. **216** (1992) 253.

[8] ALEPH Coll., "*ALEPH: a detector for electron-positron annihilations at LEP* ", Nucl. Instrum. and Methods **A294** (1990) 121;
D. Creanza *et al.*, "*The new ALEPH silicon vertex detector* ", Nucl. Instrum. and Methods **A409** (1998) 157.

[9] ALEPH Coll., "*Performance of the ALEPH detector at LEP* ", Nucl. Instrum. and Methods **A360** (1995) 481.

[10] J.F. Grivaz and F. Le Diberder, "*Complementary analysis and acceptance optimization in new particle searches* ", LAL **92–37**(1992);
ALEPH Coll., "*Mass limit for the standard model higgs boson with the full LEP1 ALEPH data sample* ", Phys. Lett. **B384** (1996) 427.

[11] S. Katsanevas and P. Moravitz, Comp. Phys. Commun. **112** (1998) 227.

[12] ALEPH Coll., "*Search for sleptons and squarks in e^+e^- collisions at 189 GeV* ", Phys. Lett. **B469** (1999) 303.

[13] T. Sjostrand, Comp. Phys. Commun. **82** (1994) 74, `CERN-TH 7112/93` (1993).

[14] J. Fujimoto et al., Comp. Phys. Commun. **100** (1997) 128.

[15] D.E. Groom *et al.,* "*Review of Particle Physics* ", Eur. Phys. J. **C15** (2000)1.

[16] F.E. Paige, S.D. Protopopescu, H. Baer and X. Tata, "*ISAJET 7.51 - A Monte Carlo event generator for pp, $p\bar{p}$ and e^+e^- reactions* ", documentation and code available from `ftp://penguin.phy.bnl.gov/pub/isajet/.`

[17] J. Ellis *et al.*, Phys. Rev. **D58** (1998) 5002.

[18] ALEPH Coll., "*Search for Gauge mediated SUSY Breaking topologies at $\sqrt{s}$ = 189 GeV*", Eur. Phys. J. **C16** (2000) 71.

[19] L3 Coll., "*Search for scalar leptons in e^+e^- collisions at $\sqrt{s}$ = 189 GeV*", Phys. Lett. **B471** (1999) 280.

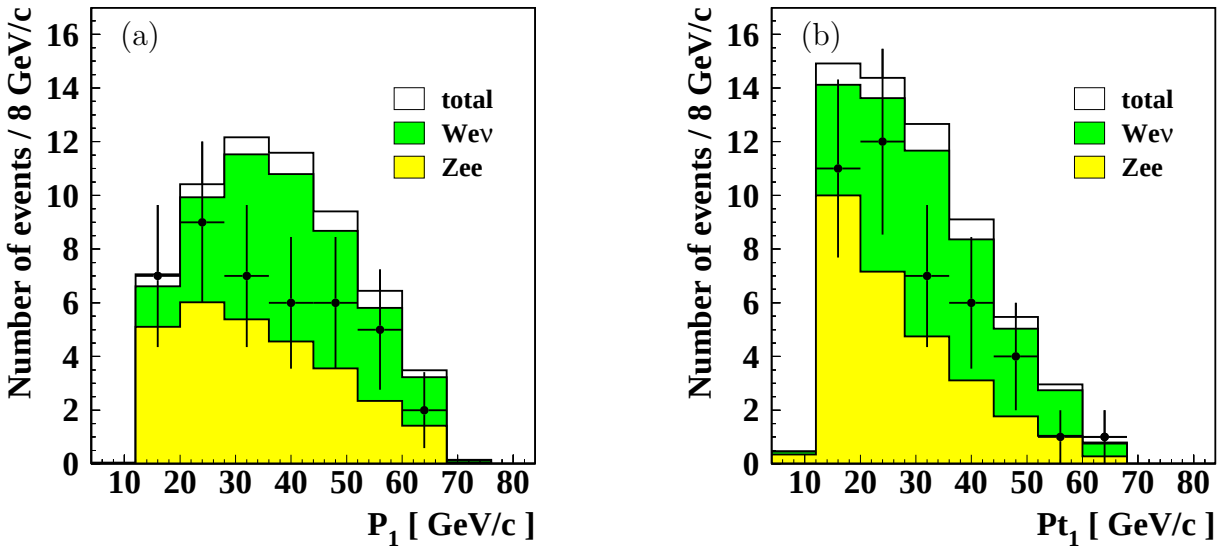

Figure 1: Comparison between data (dots with error bars) and expected backgrounds (histograms) after the single-electron selection cuts for centre-of-mass energies ranging from 189 to 209 GeV. Distributions of (a) the momentum P_1 and (b) the transverse momentum Pt_1 of the leading electron.

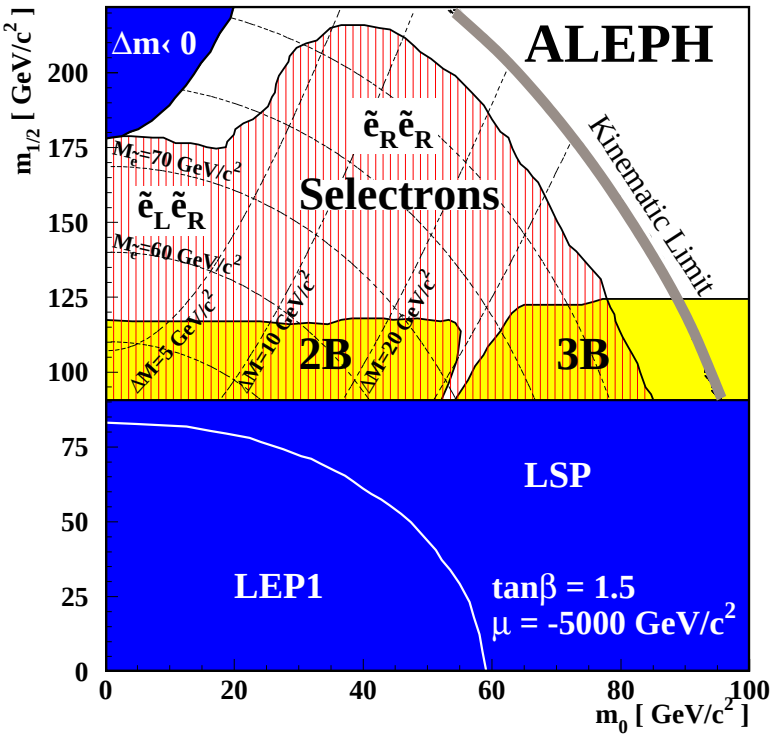

Figure 2: Regions excluded in the (m_0, $m_{1/2}$) plane by direct searches for selectrons and charginos for $\tan\beta = 1.5$ and $\mu = -5000\,\mathrm{GeV}/c^2$. The dark-shaded regions are theoretically forbidden ($\Delta M < 0$) or excluded by LEP1 [7] or the LSP limit [3]. The light-shaded regions are excluded by direct searches for chargino two-body (2B) and three-body (3B) decays [3, 4]. The hatched region is excluded by the selectron search. Lines of constant ΔM values and of constant $m_{\tilde{e}_R}$ values are also shown. The thick line indicates the kinematic limit for $\tilde{e}_R\tilde{e}_R$ production.

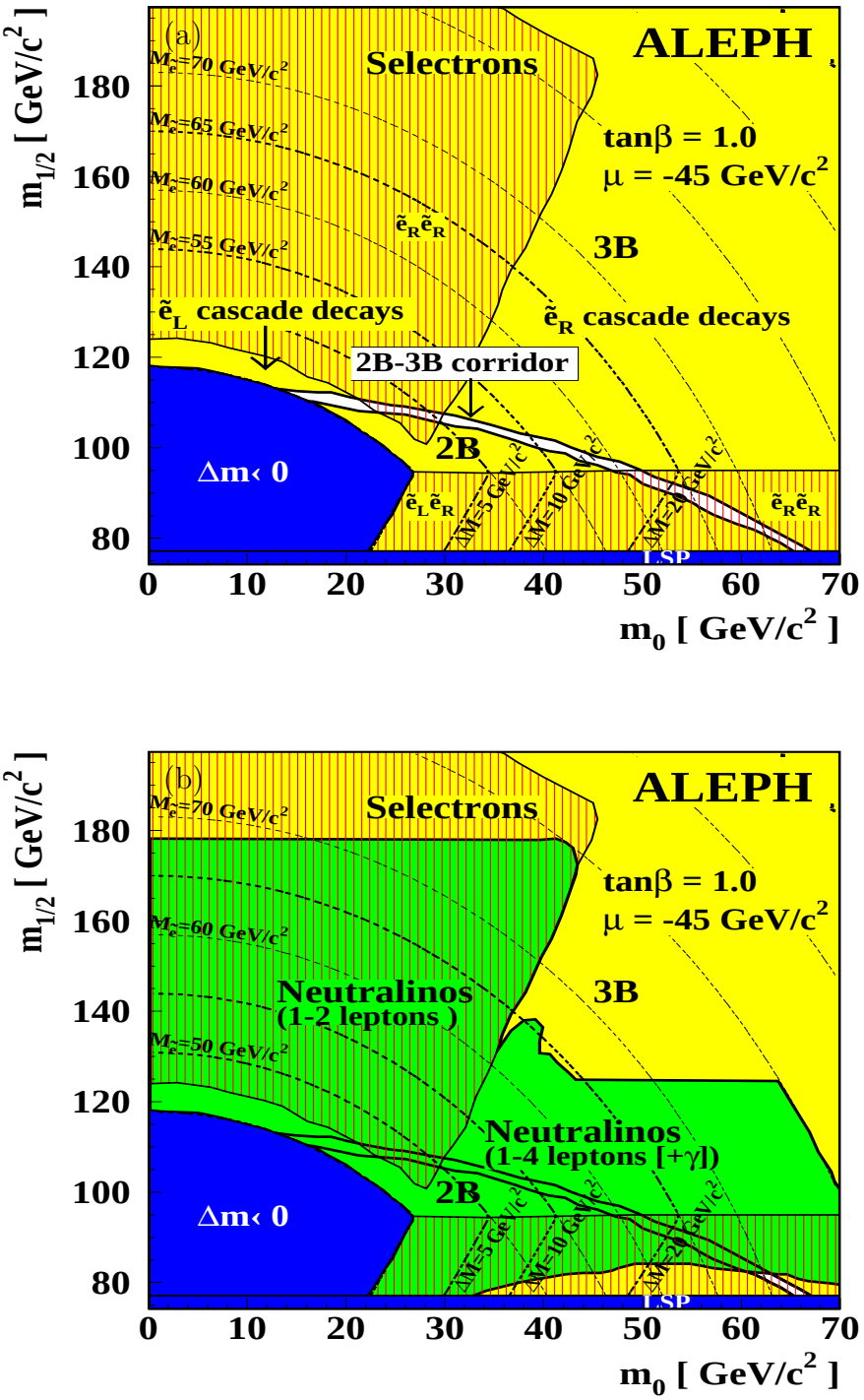

Figure 3: (a) Regions excluded in the $(m_0, m_{1/2})$ plane by direct searches for selectrons and charginos, for $\tan\beta = 1.0$ and $\mu = -45\,\mathrm{GeV}/c^2$. The selectron limit at large m_0 is a line of constant $m_{1/2}$, where the photino field content of the χ_2^0 becomes large enough for the selectrons to decay predominantly via cascades. The thin dashed curves are the lines of constant $\tilde{\mathrm{e}}_\mathrm{R}$ mass, and the thick dashed curves are the lines of constant mass difference with the LSP. Because the LSP mass does not depend on $m_{1/2}$ above $95\,\mathrm{GeV}/c^2$, the iso-ΔM lines become identical to the iso-$m_{\tilde{\mathrm{e}}_\mathrm{R}}$ lines. (b) Same as (a), including the regions that can be covered by dedicated $\chi_1^0\chi_3^0$ searches (dark shaded). The same hatching and shading conventions as in Fig. 2 are adopted.

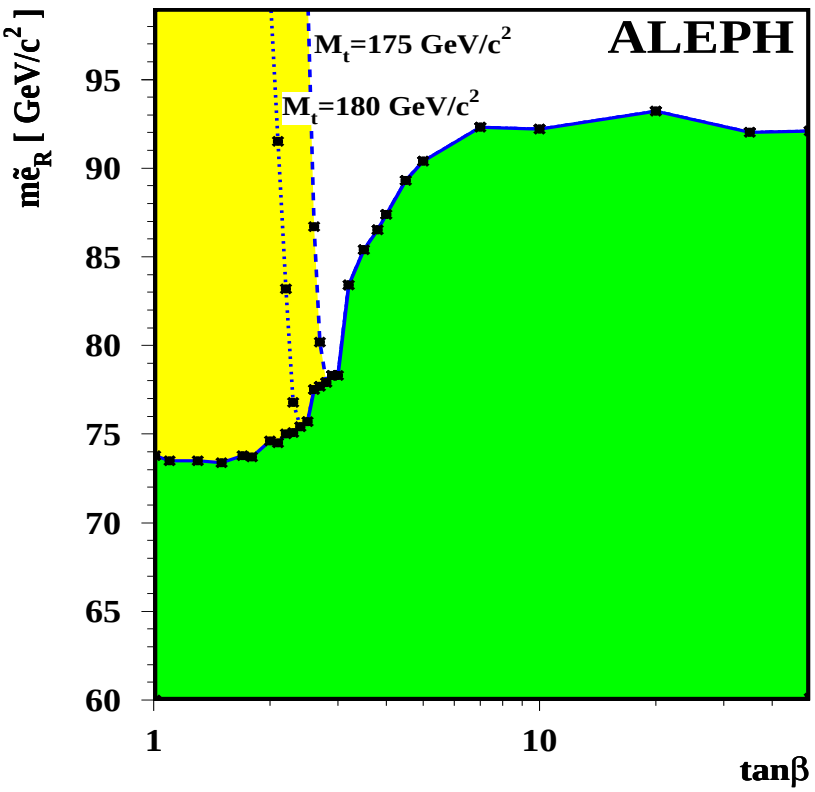

Figure 4: Limit on $m_{\tilde{e}_R}$ as a function of $\tan\beta$. The limit from the Higgs boson searches for $m_{\rm top}$=175(180) GeV/c^2 is given by the dashed(dotted) line.

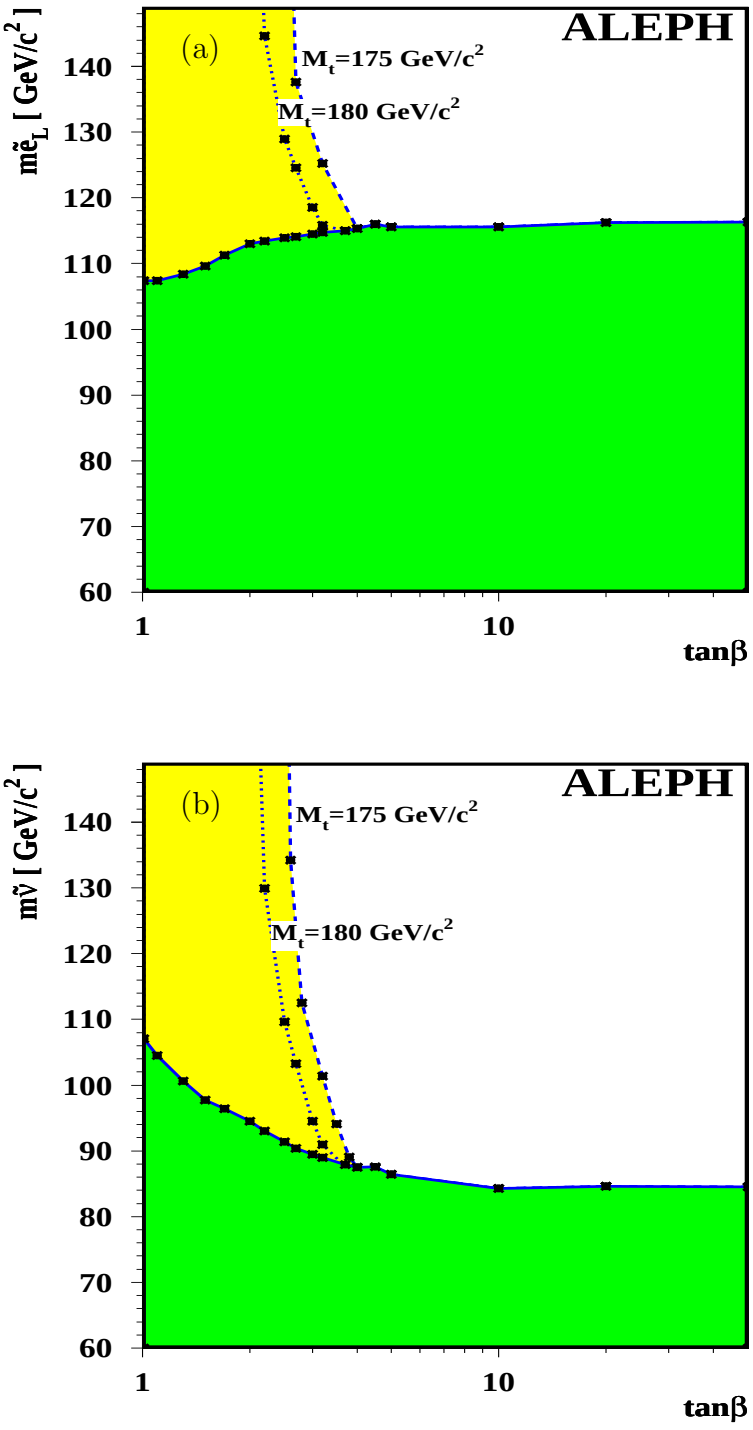

Figure 5: Limits on $m_{\tilde{e}_L}$ (a) and $m_{\tilde{\nu}}$ (b) as a function of $\tan\beta$. The limit from the Higgs boson searches for $m_{\rm top} = 175(180)\,{\rm GeV}/c^2$ is given by the dashed(dotted) line.

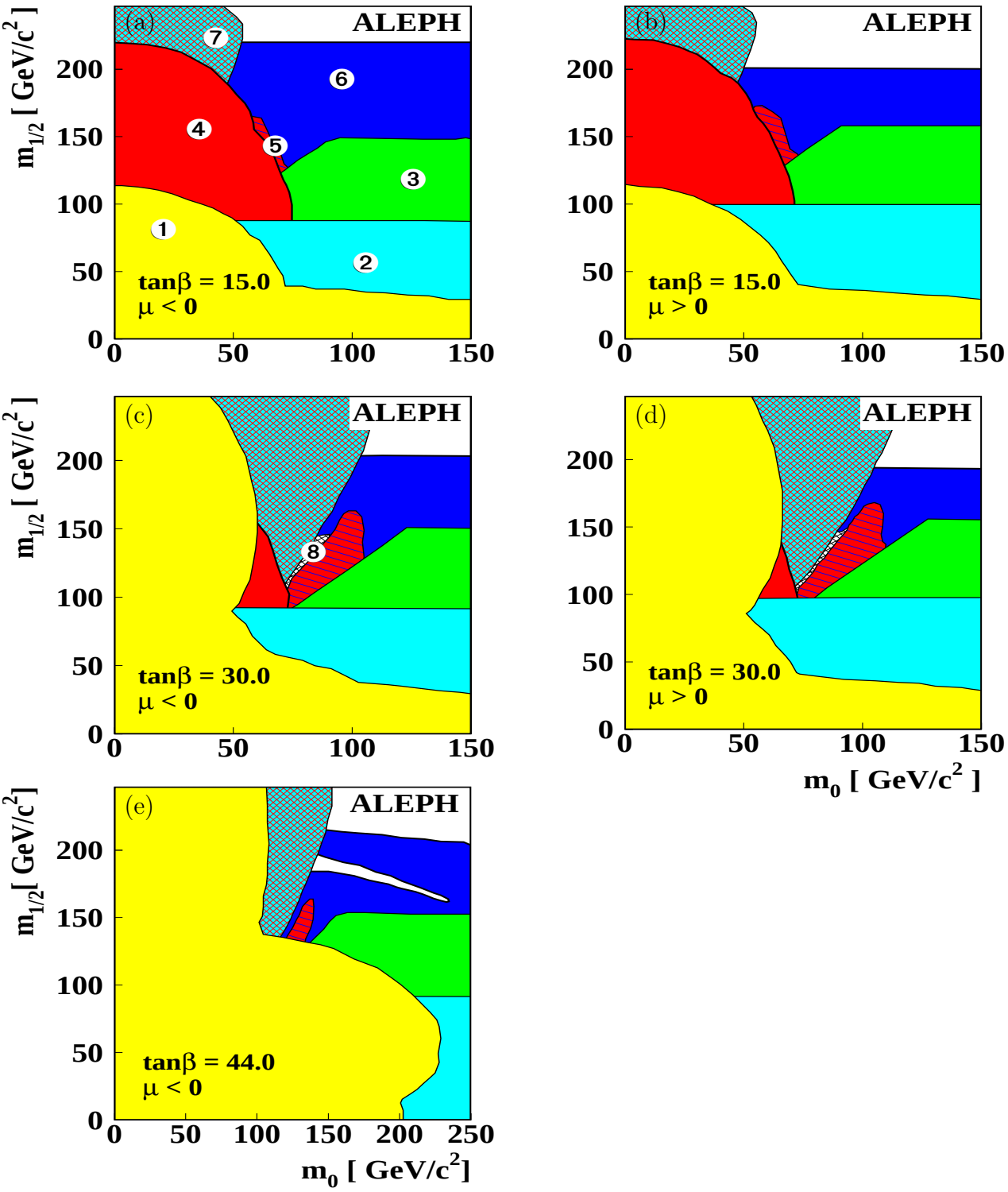

Figure 6: Minimal Supergravity scenario: regions excluded in the (m_0, $m_{1/2}$) plane for $\tan\beta = 15$, 30 and 44 and for $A_0 = 0$. Region 1 is theoretically forbidden. The other regions are excluded by LEP1 (2), and by searches for charginos (3), selectrons (4), staus (5), Higgs bosons (6), stable charged particles (7), and associated neutralino production (8).

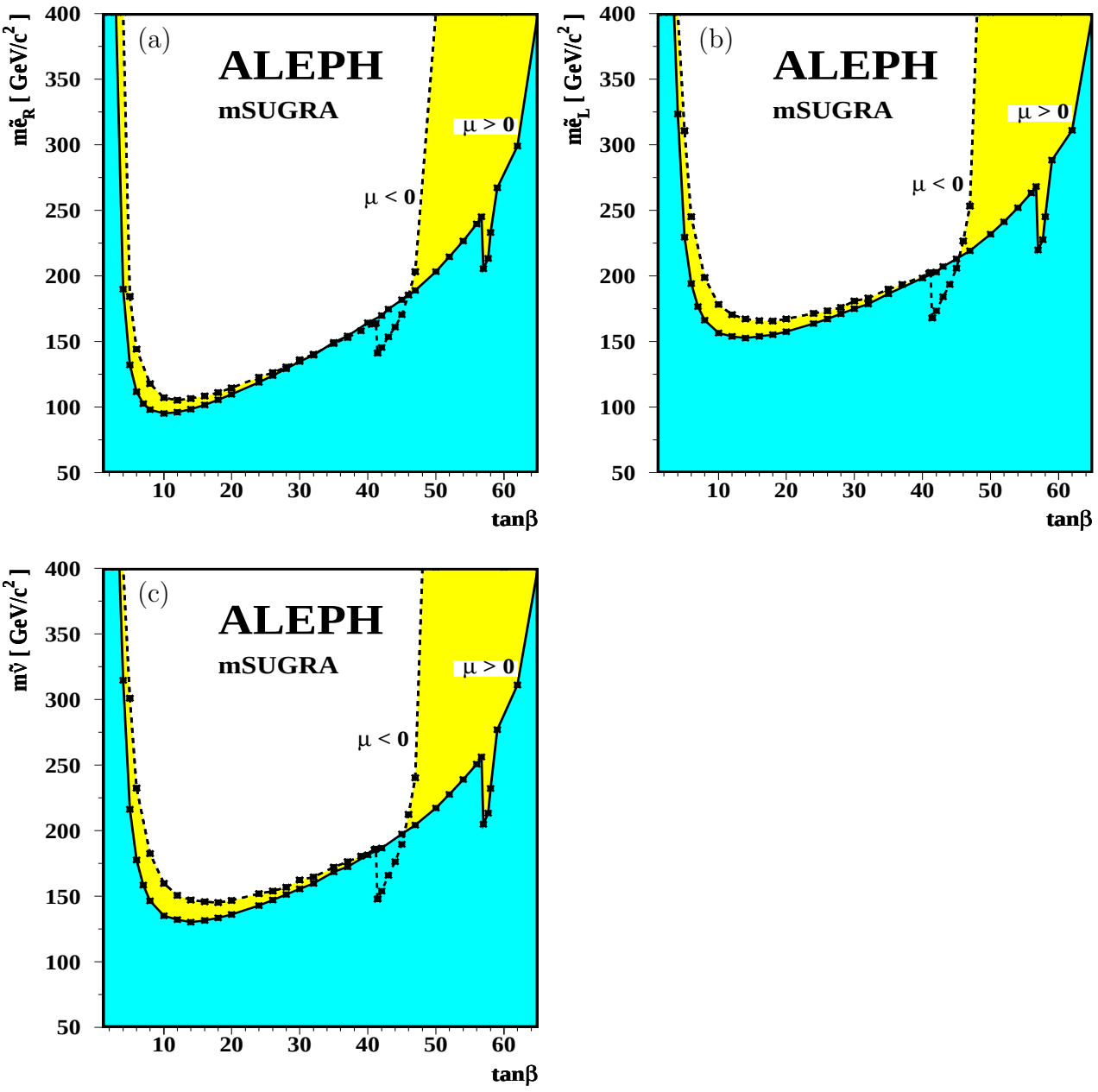

Figure 7: Limits within mSUGRA on $m_{\tilde{e}_R}$ (a), $m_{\tilde{e}_L}$ (b) and $m_{\tilde{\nu}}$ (c) as a function of $\tan\beta$ for $\mu < 0$ (dashed line) and $\mu > 0$ (full line). Detailed explanations about the structure at large $\tan\beta$ values can be found in Section 5.5.